Silicalite-1 As Efficient Catalyst for Production of Propene from 1-Butene

Palani Arudra, Tazul Islam Bhuiyan, Muhammad Naseem Akhtar, Abdullah M. Aitani, Sulaiman S. Al-Khattaf,* and Hideshi Hattori

Center of Research Excellence in Petroleum Refining and Petrochemicals, King Fahd University of Petroleum & Minerals, Dhahran 31261, Saudi Arabia

Ⓢ *Supporting Information*

ABSTRACT: Reaction of 1-butene was studied over silicalite-1 and H-ZSM-5 zeolites with different Al contents (SiO_2/Al_2O_3 molar ratio (Si/Al_2) = 23, 80, and 280) to explore an efficient catalyst for the formation of propene as well as to elucidate the reaction scheme and the relevant acid sites involved in the reaction. The formation of alkenes, including propene, increased and those of alkanes and aromatics decreased with decreasing Al content. The percentage of alkenes other than *n*-butene isomers was 60 C-wt % over silicalite-1 at 550 °C with 34.1 C-wt % propene. Over H-ZSM-5 with Si/Al_2 = 23, the formation of alkenes was negligible, and the main products were alkanes and aromatics, the sum of alkanes and aromatics being 65.4 C-wt % at 550 °C. These product distributions are consistently interpreted by the successive reactions of oligomerization, cracking, and hydrogen transfer. For oligomerization and cracking, in addition to strong acid sites on H-ZSM-5 zeolites, weak acid sites present on silicalite-1 act as active sites. For the hydrogen transfer reaction of alkenes to form alkanes and aromatics, strong acid sites are required. The scheme can also be applicable to the reactions of 1-pentene and 1-hexene. The weak acid sites on silicalite-1 are assumed to be the silanol groups that act as Brønsted acid above 300 °C. The presence of strong acid sites on H-ZSM-5 catalysts, which are the OH groups bridging to Si and Al, results in the consumption of alkenes by hydrogen transfer. Removal of a part of Al contained in silicalite-1 as an impurity and enrichment of surface silanol groups on silicalite-1 resulted in the improvement of the propene yield. It is concluded that silicalite-1 is an efficient catalyst for the formation of propene by the reactions of light alkenes because of the absence of strong acid sites and the presence of weak acid sites.

KEYWORDS: silicalite-1, H-ZSM-5, 1-butene, propene, alkene cracking, hydrogen transfer, weak acid
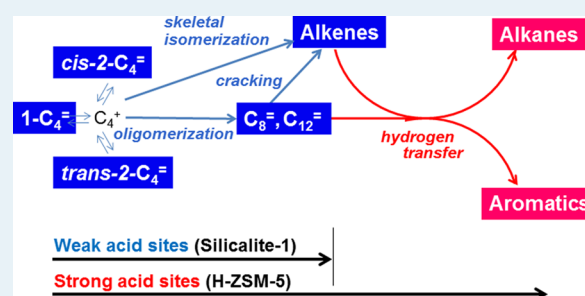
Highly selective propene production has received much attention in recent years because of its use in important derivatives of polymers, intermediates, and chemicals. The demand for propene is growing very rapidly, primarily driven by a high growth rate of polypropylene usage.[1]

Several propene production technologies have been investigated including methanol-to-olefin process, steam cracking, propane dehydrogenation, catalytic cracking of C_4-alkenes, and metathesis.[2] Among these methods, the process of butene cracking has attracted much attention because of the availability of large and stable supplies of butene isomers from FCC and stream cracking processes.[3−5] Cracking of C_4 to C_6 alkenes appears to be a promising technology for production of propene and ethylene.[6,7]

The catalysts studied so far for the purpose of propene production by cracking include H-ZSM-5, H-ZSM-48, PITQ-13, and SAPO-34.[8−15] H-ZSM-5 showed a high propene yield of 35% after modification with phosphorus and lanthanum.[8] H-ZSM-48 showed a higher propene selectivity in C_4-alkene cracking compared with H-ZSM-5, although the reasons for the high selectivity were not certain.[9]

Zhu et al. studied the effects of zeolite pore structure and Si/Al_2 ratio on the cracking of C_4 alkenes to propene.[11] A high selectivity to propene was observed for the medium-pore 10-membered ring zeolites and the small-pore SAPO zeolite. The smaller the pore size of the zeolites, the greater the extent of suppression of the hydrogen transfer reaction of alkenes and the higher the propene selectivity. The H-ZSM-5 with an Si/Al_2 ratio of 366 exhibited the best performance. Lin et al. reported that the H-ZSM-5 modified with phosphorus to reduce the number of strong acid sites showed the best performance in the reaction of 1-butene to propene.[14] They suggested that adjusting the acid site distribution is important. Zeng et al. also reported that the phosphorus-modified PITQ-13 yielded a high propene yield of 41.6 C-wt %.[15] They reported that the modification with phosphorus weakened the acid sites to result in the high yield of propene. Recently, Epelde et al. reported that K-modified H-ZSM-5 showed a high yield of propene in the reaction of 1-butene. They explained the role of K to hinder

the second reactions of aromatization and hydrogen transfer by reducing the density and strength of acid sites.[16]

Silicalite-1 has the same crystalline structure as ZSM-5, but contains no Al. The acid sites on silicalite-1 are so weak that the acid sites cannot be detected by ammonia TPD under normal conditions. Because alkenes are easily protonated to form carbocations, the weak acid sites on silicalite-1 would be able to form carbocations to initiate the acid-catalyzed reactions. Because the strength of acid sites increases with temperature, the formation of carbocations from alkene would be plausible over silicalite-1 in particular at a high temperature. To the best of our knowledge, there have been no reports in the literature in which silicalite-1 was used as a catalyst in catalytic cracking of light alkenes except for one patent.[17] In the present study, silicalite-1 was synthesized, and its catalytic activity was examined in the reactions of C_4-C_6 alkenes. It was found that silicalite-1 exhibited a higher yield of propene as compared with H-ZSM-5 zeolites with a SiO_2/Al_2O_3 molar ratio (Si/Al_2) of 23−280.

1. EXPERIMENTAL METHODS

1.1. Reagents. Tetrapropylammonium bromide (98%), ammonium fluoride (98%), fumed silica (Cab-O-sil M-5) (99.8%), 1-pentene (98.5%), and 1-hexene (97%) were purchased from Sigma-Aldrich and used without further purification. 1-Butene (99.9%) was procured from Saudi Industrial Gas Company.

1.2. Catalyst Synthesis. H-ZSM-5 zeolites with Si/Al_2 molar ratios of 23, 80, and 280 were obtained by calcination of the ammonium forms of the ZSM-5 zeolites purchased from Zeolyst International at 500 °C for 2 h in air and are denoted by H-ZSM-5(23), H-ZSM-5(80), and H-ZSM-5(280), respectively.

Silicalite-1 was synthesized according to the procedures reported in the literature.[18] In a typical synthesis, 4.26 g of tetrapropylammonium bromide (TPABr) and 0.74 g of ammonium fluoride (NH_4F) were dissolved into 72 mL of water. Then, 12 g of fumed silica was added, and the mixture was stirred until a homogeneous gel was formed. The gel was subjected to a hydrothermal crystallization process at 200 °C for 2 days. The molar composition of the gel was 1 SiO_2/0.08 TPABr/0.10 NH_4F/20 H_2O. The gel was washed with water and dried at 80 °C overnight. The template was removed by calcination at 750 °C for 6 h in air.

Because silicalite-1 normally contains a trace amount of Al that originates from impurity in a Si source, we prepared the HCl-treated silicalite-1, which is supposed to have a smaller amount of Al. For the HCl-treated silicalite-1, silicalite-1 (5 g) was mixed with 100 g of 1 M HCl aqueous solution. The mixture was stirred for 24 h under reflux conditions. The sample was filtered, washed with deionized water, and dried at 100 °C for 4 h, followed by calcination at 550 °C for 5 h in air. The HCl-treated silicalite-1 was denoted by silicalite-1(HCl).

We also prepared NH_3-treated silicalite-1, which is supposed to have a larger number of the surface OH groups. For the NH_3-treated silicalite-1, silicalite-1 (4 g) was mixed with 20 g of a mixture of aqueous solutions of ammonia (10 g, 25 wt %) and ammonium nitrate (10 g, 7.5 wt %) in a glass beaker. This mixture was transferred into a polypropylene bottle and stirred at 90 °C under autogenous pressure for 1 h. The catalyst was then washed with deionized water, filtered, and dried at 110 °C for 4 h, followed by calcination at 550 °C for 5 h in air. The NH_3 treated sample was denoted by silicalite-1(NH_3).

Because silicalite-1 was prepared with NH_4F, a trace amount of F might be included in the resulting silicalite-1. To examine the effect of F, we prepared silicalite-1 without using a compound containing F according to the literature.[19] In a typical synthesis, 6 g of fumed silica was mixed with tetrapropylammonium hydroxide (TPAOH) and water. The resulting mixture was crystallized for 4 days at 90 °C. The composition of the gel was 1.0 SiO_2/0.085 TPAOH/3.72 H_2O. After crystallization, the product was mixed with water and centrifuged. The obtained solid was dried at 90 °C for 12 h and calcined at 750 °C for 6 h. The silicalite-1 prepared by this method was denoted by silicalite-1(non-F).

1.3. Catalyst Characterization. The elemental analysis for Si and Al was performed by ICP-OES with an optical emission spectrometer, Ultima 2, Horiba Scientific. In a typical procedure, 50 mg of catalyst sample was fused with 300 mg of lithium metaborate in a muffle furnace at 950 °C for 15 min. The fused product was dissolved in 20 mL of 4% HNO_3 and diluted with deionized water to make a total volume of 50 mL. The obtained solution was analyzed by ICP-OES.

The F content in silicalite-1 was measured by ion-exchange chromatograpy. Silicalite-1 (50 mg) was fused with lithiummetaborate, dissolved into 50 mL of KOH aqueous solution and analyzed by ion-exchange chromatography. The content of F in silicalite-1 was 0.000 01 wt % (0.1 ppm).

The zeolite samples were characterized by X-ray powder diffraction (XRD) with a Rigaku Mini-flex II system using nickel filtered Cu $K\alpha$ radiation (λ = 1.5406 Å, 30 kV, and 15 mA). The XRD patterns were recorded in static scanning mode from 1.2 to 50° (2θ) at a detector angular speed of $2°$ min^{-1} with a step size of 0.02°. The crystal size was estimated by Scherrer's method for the peak at $2\theta \sim 7.9°$ for diffraction of the (011) face.

The surface areas of the catalyst sample were measured by nitrogen adsorption at −195 °C with Autosorb-1 (Quanta Chrome), the BET equation being applied to the isotherm. The external surface area was estimated from a t-plot.

SEM images were measured with a JEOL JSM-5800 scanning microscope. Magnification was 7000. Before taking SEM photographs, the samples were loaded onto a sample holder, held with conductive aluminum tape, and coated with a film of gold in vacuo using a cressington sputter ion-coater for 20 s with 15 mA current.

The IR spectra of pyridine adsorbed on the sample were measured for Brønsted acid sites and Lewis acid sites. The thin wafer sample was pretreated at 450 °C in a vacuum. After cooling to room temperature, the sample was exposed to pyridine at room temperature for 5 min and evacuated at 150 °C for 30 min. IR spectra were measured at room temperature.

IR spectra of the silicalite-1, silicalite-1(HCl), and silicalite-1(NH_3) in the OH stretching region were measured for the wafer samples disks prepared with KBr because self-supporting wafer transparent to IR light could not be made without KBr. The sample in the form of a self-supporting wafer was prepared using 15 mg of sample mixed with 85 mg of KBr. The diameter of wafer was ∼20 mm. The wafer was then placed in an in situ cell (Makuhari Rikagaku Garasu Inc., JAPAN) and pretreated under a vacuum (∼2 × 10^{-1} Pa) at 300 °C for 1 h. All spectra were measured at room temperature with Nicolet FTIR spectrometer (Magna 500 model).

Temperature-programmed desorption (TPD) of ammonia was performed with a BEL-CAT-A-200 chemisorption apparatus. The measurement conditions were the same as those proposed

by Katada et al.[20] The sample (100 mg) was pretreated at 500 °C under a helium flow for 60 min, followed by exposure to ammonia at 100 °C. The ammonia excessively adsorbed was flushed by a helium stream for 30 min at 100 °C. TPD was run from 100 to 600 °C at a ramp rate of 10 °C min^{-1}. Those TPD measurement conditions are suitable to measure the strong acid sites on zeolites. To measure the weak acid sites, three experiments in which the flushing temperature was set at 25 °C were carried out for silicalite-1, silicalite-1(HCl), and silicalite-1(NH$_3$).

1.4. Reaction Procedures. The catalytic cracking of C$_4$−C$_6$ alkenes was performed in a fixed-bed tubular reactor packed with 2 mL of catalyst with a particle size of 0.5−1.0 mm diameter, which was sandwiched between 6 and 2 mL of SiC particles. The catalyst sample was pretreated in a nitrogen stream at 550 °C for 1 h, and then a mixture of the feed and nitrogen (5 mL/min and 25 mL/min, respectively) (GHSV = 900 h^{-1}) was passed through the catalyst bed at 550 °C. For the reaction of 1-butene, the reaction temperature was varied in a range of 50−550 °C. The products were analyzed by online GC equipped with a GS-Gaspro column and a flame ionization detector (FID).

2. RESULTS AND DISCUSSION

2.1. Catalyst Characterization. XRD patterns of silicalite-1 and H-ZSM-5 zeolites are presented in Figure 1. All samples exhibited characteristic peaks of MFI structure in the ranges
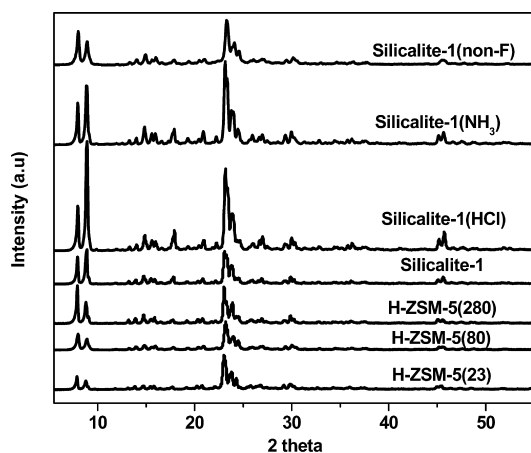
2θ = 7−10° and 22−25°.[21−24] The relative intensity of diffraction peaks was different, depending on the sample. This is caused by a difference in crystal growth for the different samples. The first peak observed at about 2θ = 7.9° is a superposition of the diffractions from (−101), (011), and (101) faces, diffraction from the (011) face being the main peak. The second peak observed at about 2θ = 8.9° is a superposition of the diffraction from the (020), (200), (−111), and (111) faces, the diffractions from the (020) and (200) faces being dominant. From the similarity of the relative peak intensity, the crystal growth for silicalite(non-F) is the same as those of H-ZSM-5's. Crystal sizes estimated by Scherrer's method for the peak at about 2θ = 7.9° (011) face are presented in Table 1.

SEM images of all samples are shown in Figure 2. Particles were larger as the Si/Al$_2$ ratio increased for H-ZSM-5's. The image for H-ZSM-5 showed relatively large quadrangular prismlike crystallites. Silicalite-1, silicalite-1(HCl), and silicalite-1(NH$_3$) showed a mixture of large crystallites and small particles. Silicalite-1(non-F) was composed of only small particles. Because Scherrer's method to obtain crystal size cannot applied to crystals larger than 0.1−0.2 μm, the values of crystal size listed in Table 1 do reflect the large crystallites observed for silicalite-1, silicalite-1(HCl), and silicalite-1(NH$_3$).

The BET and external surface areas of the samples are presented in Table 1. The surface areas were not much different for all samples, although the surface areas of H-ZSM-5's and silicalite-1(non-F) were ≥400 m^2 g^{-1}, and those of silicalite-1, silicalite-1(HCl) and silicalite-1(NH$_3$) were <400 m^2 g^{-1}. A large difference was observed in the external surface area. Silicalite-1(non-F) showed a high external surface area of 122 m^2 g^{-1}, whereas H-ZSM-5's showed decreasing surface areas of 82−33 m^2 g^{-1} with an increase in the Si/Al$_2$ ratio. Low external surface areas were observed for silicalite-1, silicalite-1(HCl), and silicalite-1(NH$_3$). This is consistent with the SEM images; large crystallites were observed for the samples with low external surface areas.

Figure 3 shows the FT-IR spectra of the catalysts recorded after the adsorption of pyridine and subsequent evacuation at 150 °C. The absorption bands at 1545 and 1455 cm^{-1} were assigned to the pyridinium ion formed on the Brønsted acid site and pyridine coordinated to Lewis acid sites, respectively.[25] The numbers of Lewis and Brønsted acid sites were highest for H-ZSM-5(23) as compared with other zeolites (Table 1). With silicalite-1, no absorption peaks were appreciable. There remained a negligible amount of pyridine after evacuation of preadsorbed pyridine at 150 °C.


Figure 1. XRD patterns of H-ZSM-5(23), H-ZSM-5(80), H-ZSM-5(280), silicalite-1, silicalite-1(HCl), silicalite-1(NH$_3$), and silicalite-1(non-F).

Table 1. Physicochemical Characterization of H-ZSM-5 with Different Si/Al$_2$ Ratios and Silicalite-1

| sample	d (011) (Å)^a	crystal size^b (Å)	Si/Al$_2$ molar ratio^c	surface area BET/ext. SA by t-plot (m^2 g^{-1})	NH$_3$-TPD^d (mmol g^{-1})	pyridine FT-IR (mmol g^{-1})^e		
						TA	B	L
H-ZSM-5(23)	12.09	426	2.4×10	425/82	0.25	0.79	0.69	0.10
H-ZSM-5(80)	11.83	313	8.6×10	425/68	0.16	0.14	0.08	0.06
H-ZSM-5(280)	11.89	423	2.95×10^2	400/33	0.07	0.02	0.01	0.01
silicalite-1	11.94	457	2.17×10^3	348/5.0	nd	nd	nd	nd
silicalite-1(HCl)	12.00	437	2.50×10^3	374/6.8	na	na	na	na
silicalite-1(NH$_3$)	12.00	458	2.04×10^3	295/4.7	na	na	na	na
silicalite-1(non-F)	11.78	341	1.95×10^3	446/122	na	na	na	na

^{a}Evaluated by XRD peak at about 2θ = 7.9. ^{b}Calculated by Scherrer's method using peak at about 2θ = 7.9. ^{c}Si/Al$_2$ molar ratio by ICP analysis. ^{d}Acidity calculated using high-temperature NH$_3$ desorption peak. ^{e}Absorptivity ratio $\varepsilon_{1455}/\varepsilon_{1545}$ = 1.33 was used to calculate the acidity.[26] TA = total acidity, B = Brønsted acidity, L = Lewis acidity, nd = not detectable, na = not available.
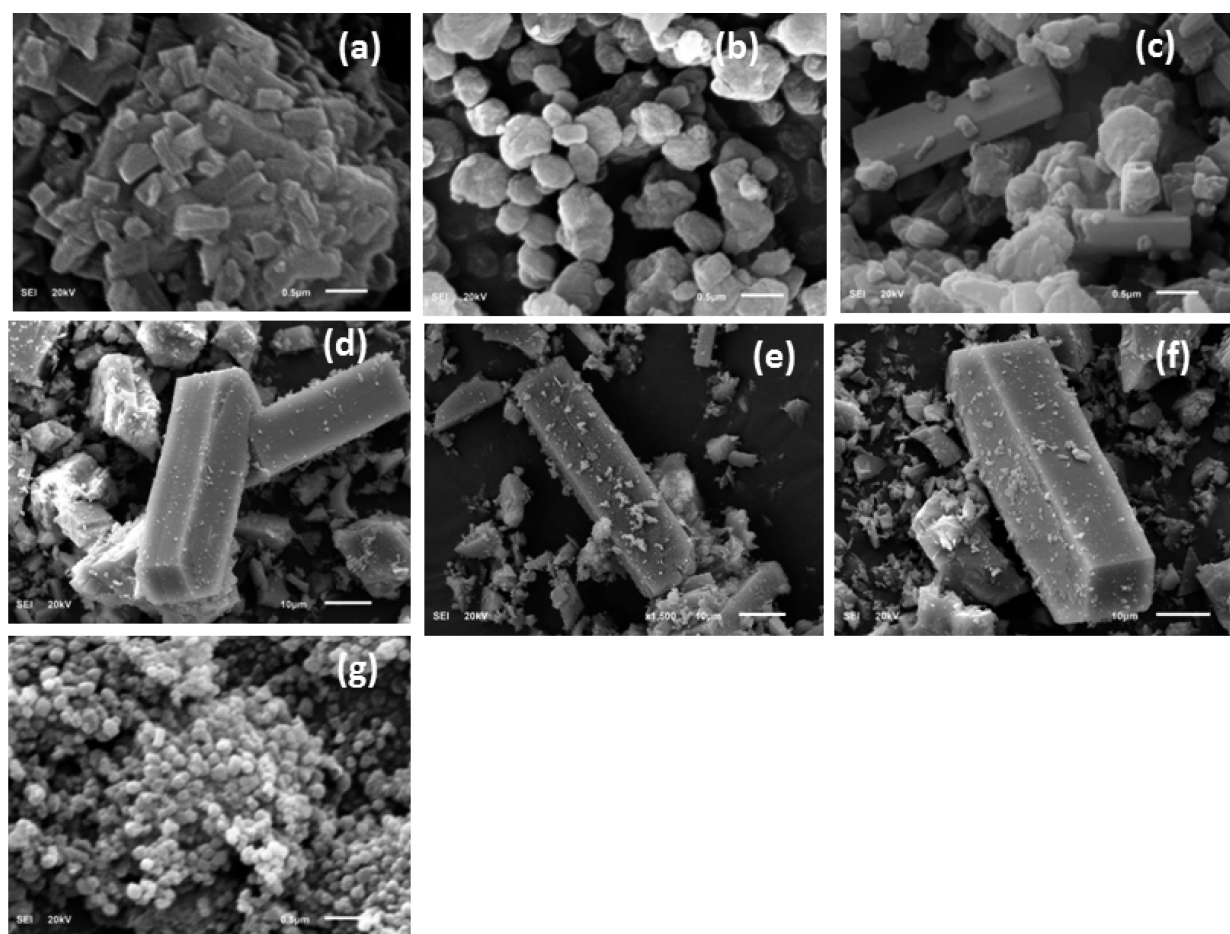
Figure 2. SEM images of (a) H-ZSM-5(23), (b) H-ZSM-5(80), (c) H-ZSM-5(280), (d) silicalite-1, (e) silicalite-1(HCl), (f) silicalite-1(NH₃), and (g) silicalite-1(non-F).
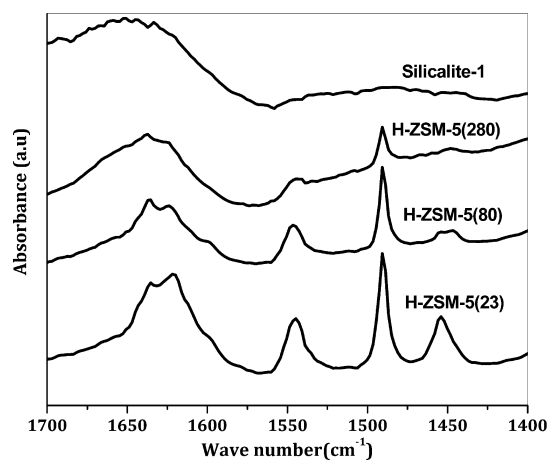
Figure 3. FT-IR spectra of pyridine adsorbed on H-ZSM-5(23), H-ZSM-5(80), H-ZSM-5(280), and silicalite-1 and subsequent outgassing at 150 °C.
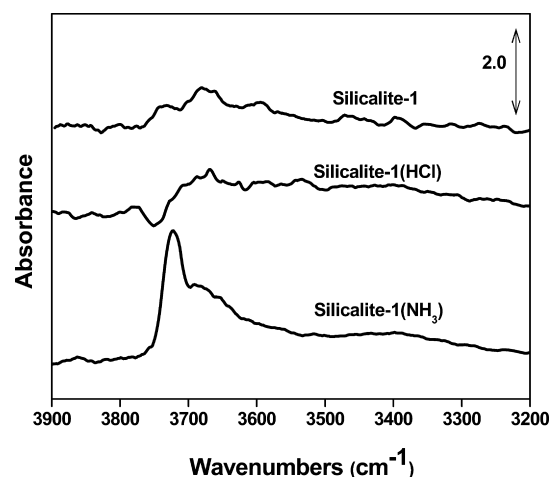

Figure 4. FT-IR spectra of silicalite-1 (a) and silicalite-1(NH₃) (b) in the OH stretching region after pretreatment at 300 °C in a vacuum.

Figure 4 shows the FT-IR spectra in the OH stretching region for silicalite-1, silicalite-1(HCl), and silicalite-1(NH₃). A band at 3725 cm^{-1} is assigned to the terminal (isolated) silanol groups, and broad bands in the range 3700−3300 cm^{-1}, to the vicinal and nest silanol groups.[26] It is evident that treatment with NH₃ increased the number of the OH groups on the surface of silicalite-1, which is in accordance with the results reported.[27] Treatment with HCl, however, did not increase the

number of the OH groups to such an extent as the treatment with NH₃.

TPD profiles of desorbed ammonia are presented in Figure 5. Two peaks appeared for H-ZSM-5 zeolites. The peaks appearing at a higher temperature correspond to the ammonia desorbed from the acid sites of zeolites. The peaks appearing at a lower temperature were assigned to ammonia molecules adsorbed either on NH₄$^{+}$ species formed on Brønsted acid sites
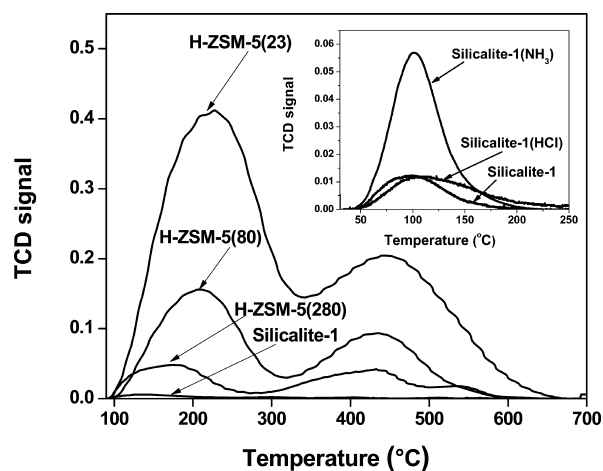
Figure 5. NH$_3$-TPD profiles of H-ZSM-5(23), H-ZSM-5(80), H-ZSM-5(280), and silicalite-1 after flushing excess NH$_3$ at 100 °C. Inset: TPD profiles of silicalite-1, silicalite-1(HCl), and silicalite-1(NH$_3$) after flushing excess NH$_3$ at 25 °C.

or on Na$^+$ cations.[28] From the areas of the peaks at a higher temperature, the numbers of acid sites were estimated and are given in Table 1. The number of acid sites increased with a decrease in the Si/Al$_2$ ratio of H-ZSM-5 zeolites, which was expected. No desorption peaks were observed in the high temperature range for silicalite-1. Because the TPD measurement conditions were suitable for measurement of strong acid sites present on zeolites, no peak for silicalite-1 indicated that no acid sites existed on silicalite-1 that were as strong as those on zeolites.

We measured the ammonia TPD under the conditions that can detect the ammonia adsorbed on weakly acidic sites. The temperature at which preadsorbed ammonia molecules were flushed with a helium flow was lowered to 25 °C, and TPD was measured for silicalite-1, silicalite-1(HCl), and silicalite-1(NH$_3$). The TPD profiles are shown in the inset of Figure 5. TPD peaks appeared at ∼100 °C, which indicated the existence of the sites that weakly adsorbed ammonia and desorbed at ∼100 °C on the surfaces of these samples. The numbers of the sites weakly adsorbing ammonia were 0.028, 0.042, and 0.174 mmol g^{-1} for silicalite-1, silicalite-1(HCl), and silicalite-1(NH$_3$), respectively.

ICP-AES analysis showed that the silicalite-1 contained 400 ppm of Al as an impurity. This corresponds to the Si/Al$_2$ molar ratio of 2.17×10^3. There might be a small number of strong acid sites, but these strong acid sites on silicalite-1 were below the detection limit by the pyridine-IR and the ammonia-TPD under normal conditions. The Si/Al$_2$ molar ratios of silicalite-1(HCl) and silicalite-1(NH$_3$) were 2.50×10^3 and 2.04×10^3, respectively. By treatment with HCl, the Si/Al$_2$ ratio increased only 15%. By treatment with NH$_3$, the Si/Al$_2$ ratio decreased, indicating that desilication occurred to some extent. The Si/Al$_2$ ratio of silicalite-1(non-F) was 1.95×10^3.

2.2. Catalytic Reactions. *2.2.1. Reaction of 1-Butene.* Because we used SiC for supporting the catalyst in the catalyst bed, we carried out a blank test in which 8 mL of SiC was placed in the reactor without catalyst (Supporting Information Table S1). Only double bond isomerization took place to a small extent. At a reaction temperature of 250 °C, no reaction occurred with SiC, whereas the conversion of 1-butene was 85% with silicalite-1. At 550 °C, 1-butene converted only to *trans*- and *cis*-2-butene by 30%, but with silicalite-1, 92% of 1-butene converted to 2-butene isomers, other alkenes, alkanes,

aromatics, and hydrocarbons heavier than C8. Therefore, the contribution of the SiC used for supporting the catalyst in the catalyst bed to the composition of the product was neglected.

In the catalytic reaction, more than 20 hydrocarbons were produced. To simplify the presentation, the products were classified into seven groups according to the expected pathway to form different products. These groups were 1-butene (reactant), *cis*- and *trans*-2-butene (double-bond isomerization products), propene (target product), alkenes other than propene and *n*-butene isomers (skeletal isomerization and cracking products), alkanes (hydrogen transfer products), aromatics (benzene, toluene, xylenes, and ethylbenzene; hydrogen transfer products), and hydrocarbons with a carbon number >8 (C8+, aromatics other than benzene, toluene, xylenes, and ethylbenzene, alkanes, and alkenes; oligomerization and hydrogen transfer products).

The changes in the compositions of propene and the aromatics as a function of the time on-stream are shown in Figure 6 for H-ZSM-5(23) and silicalite-1. The changes in the
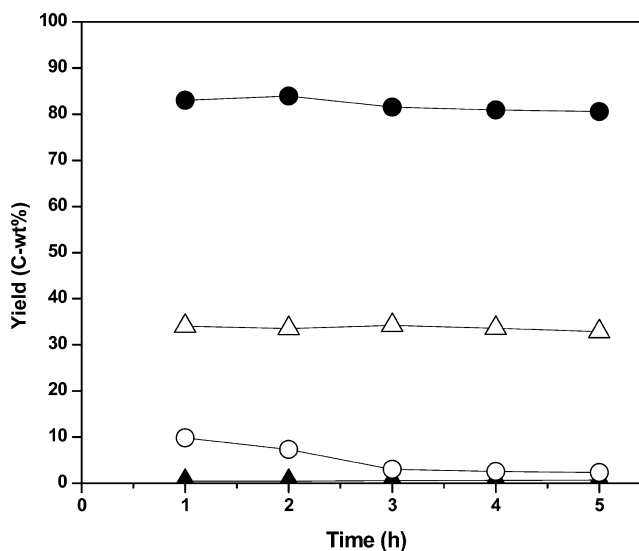

Figure 6. Variations in the yields of propene and aromatics as a function of time on-stream at 550 °C, GHSV = 900 h^{-1}. Propene over silicalite-1 (△) and H-ZSM-5(23) (▲), aromatics over silicalite-1 (○) and H-ZSM-5(23) (●).

composition with time on-stream were small for the time on-stream of 1−5 h. The activity decay was small, except for the production of aromatics over silicalite-1 on which the production of aromatics decreased during the initial 3 h.

The compositions of the grouped products are plotted against the reaction temperature and shown in Figures 7−13 for H-ZSM-5(23), H-ZSM-5(80), H-ZSM-5(280), silicalite-1, silicalite-1(HCl) and silicatlite-1(NH$_3$), and silicalite-1(non-F), respectively. The changes in the composition with reaction temperature varied with the type of catalysts. Numerical data are presented in the Supporting Information (Table S2−S8).

Over H-ZSM-5(23), double bond isomerization mainly occurred in the temperature range 50−200 °C. At 250 °C, the main products became alkenes, and C$_8$+. As the reaction temperature increased to 350 °C, the formation of alkenes became very small, and the formation of alkanes and aromatics became dominant. The dominant formation of alkanes and aromatics continued up to 550 °C, and the sum of alkanes and aromatics reached 65.4%. The formation of propene was
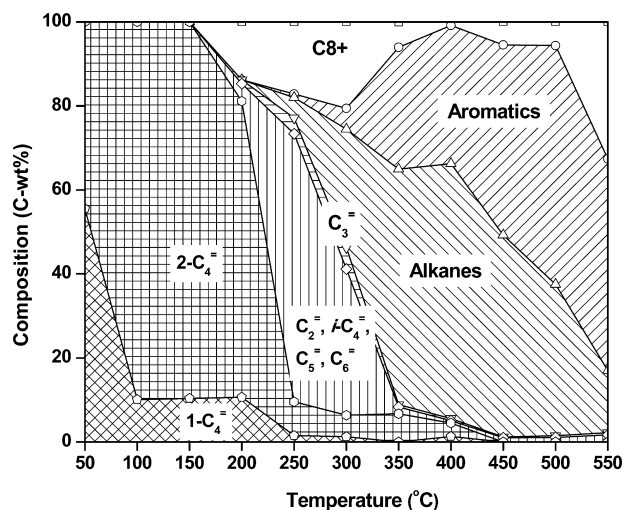
Figure 7. Variation in the composition of the products as a function of temperature for the reaction of 1-butene over H-ZSM-5(23). Aromatics, (benzene + toluene + xylene + ethylbenzene); C8+ (hydrocarbons containing more than 8 carbons, including aromatics, alkenes, and alkanes) GHSV = 900 h^{-1}; time on-stream = 1 h; total pressure, atmospheric pressure.
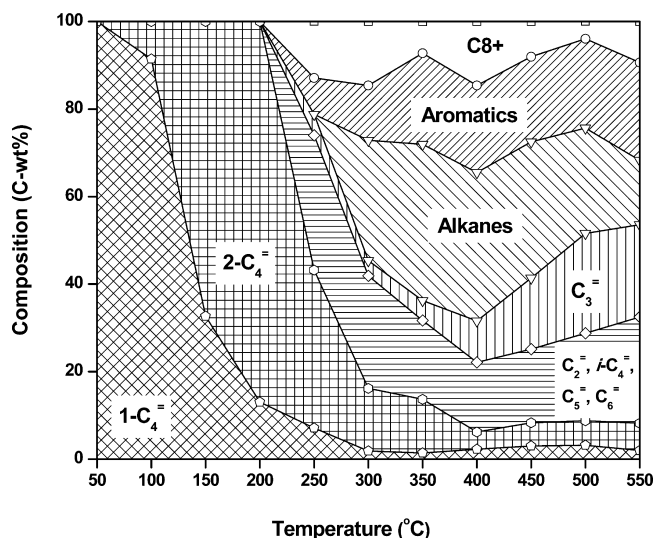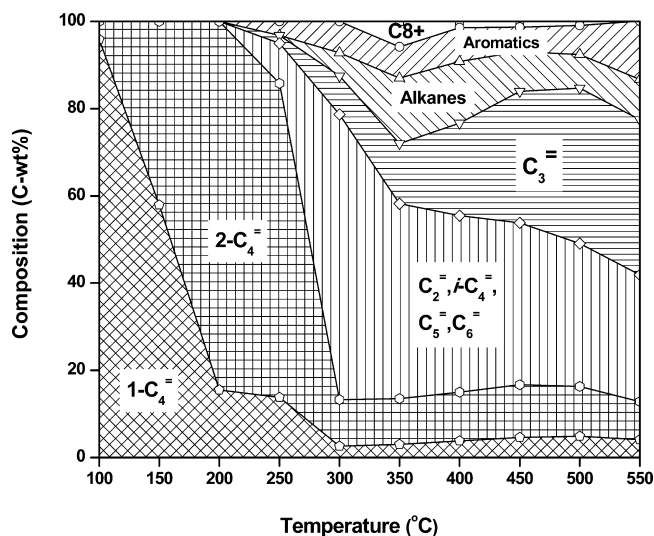

Figure 9. Variation in the composition of the products as a function of temperature for the reaction of 1-butene over H-ZSM-5(280). Expressions of compounds and reaction conditions are the same as those in Figure 7.
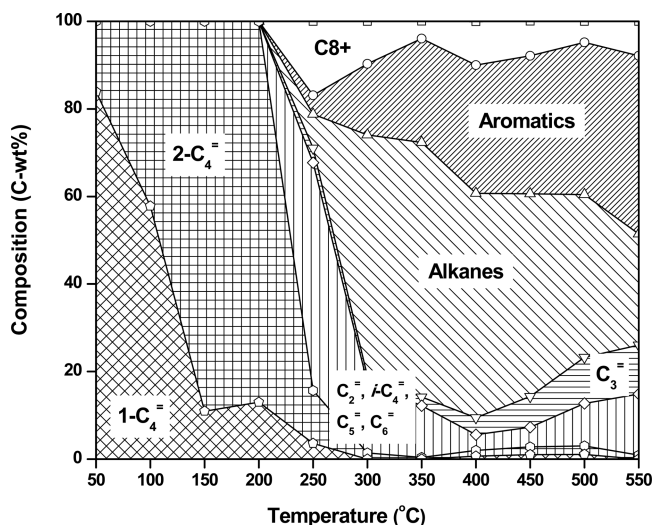
Figure 8. Variation in the composition of the products as a function of temperature for the reaction of 1-butene over H-ZSM-5(80). Expressions of compounds and reaction conditions are the same as those in Figure 7.
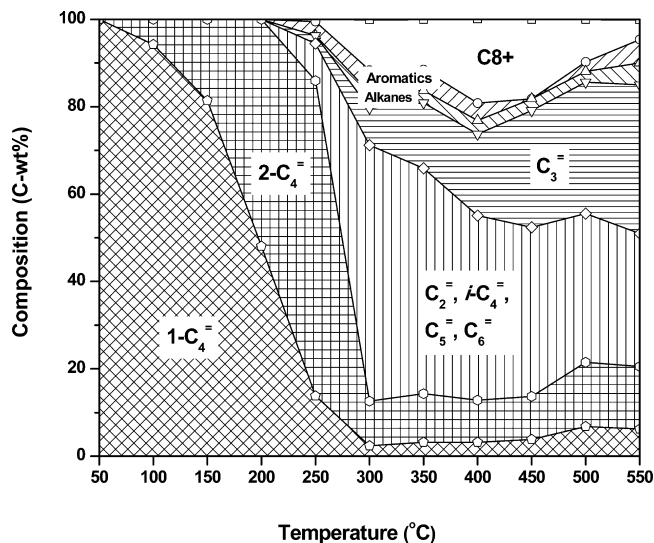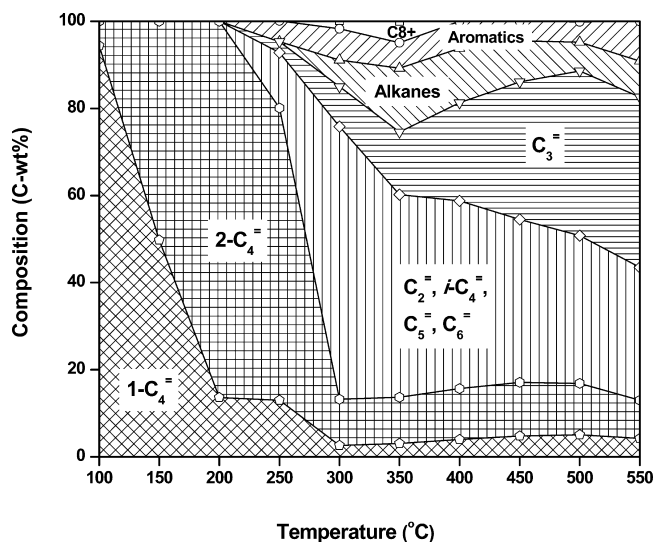

Figure 10. Variation in the composition of the products as a function of temperature for the reaction of 1-butene over silicalite-1. Expressions of compounds and reaction conditions are the same as those in Figure 7.

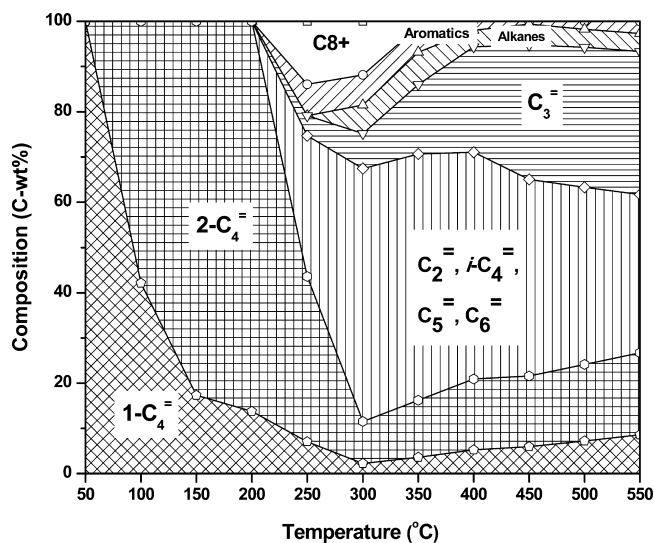observed in the temperature range 250−350 °C, but the compositions were <5%.

Over silicalite-1, no reaction was appreciable at 50 °C. In the range 100−200 °C, only double-bond isomerization occurred. At 250 °C, the main products were still 2-butene isomers. As the temperature increased to 300 °C, the formation of alkenes became predominant, and the formation of C$_8$+ occurred to some extent. The formations of alkanes and aromatics were limited to small percentages. As the reaction temperature increased further, the compositions of alkenes including propene, C$_8$+, total alkanes and aromatics did not change much; however, the percentage of propene in alkenes steadily increased and reached a maximum percentage of 34.1% of the total products at 550 °C.

Over silicalite-1(HCl), the changes in composition with temperature were similar to those over silicalite-1, although small

differences were apparent. In the temperature range 50−200 °C, double-bond isomerization occurred faster over silicalite-1(HCl) than over silicalite-1. Above 250 °C, the changes in composition as a function of temperature were similar to those for silicalite-1. Over silicalite-1(HCl), the yield of propene reached 35.6 C-wt % at 550 °C. The formation of C$_8$+, including alkenes, alkanes, and aromatics was smaller over silicalite-1(HCl) than over silicalite-1.

Over silicalite-1(NH$_3$), the changes in composition with temperature were similar to those over silicalite-1 and silicalite-1(HCl). In the temperature range 50−200 °C, double-bond isomerization occurred faster over silicalite-1(NH$_3$) than over silicalite-1, but at a rate similar to that over silicalite-1(HCl). Above 250 °C, the changes in composition as a function of temperature were similar for silicalite-1(NH$_3$), silicalite-1(HCl), and silicalite-1. Over silicalite-1(NH$_3$), the yield of

Figure 11. Variation in the composition of the products as a function of temperature for the reaction of 1-butene over silicalite-1(HCl). Expression of compounds and reaction conditions are the same as those in Figure 7.
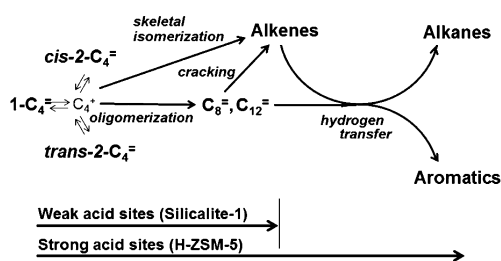

Figure 13. Variation in the composition of the products as a function of temperature for the reaction of 1-butene over silicalite-1(non-F). Expressions of compounds and reaction conditions are the same as those in Figure 7.

of H-ZSM-5(23) and silicalite-1. The change for H-ZSM-5(80) was close to that observed for H-ZSM-5(23), and the change for H-ZSM-5(280) was close to that observed for silicalite-1. The formations of alkanes and aromatics were dominant for H-ZSM-5(80) in the temperature range 300−550 °C, whereas the formations of alkenes, including propene, were dominant for H-ZSM-5(280). The percentage of propene in alkenes over H-ZSM-5(280) increased with the reaction temperature up to 500 °C. The maximum propene formation with H-ZSM-5(280) was 22.8% at 500 °C, which was close to those of alkanes and aromatics.

The changes in product distribution as a function of reaction temperature shown in Figures 7−13 suggest that the reactions of 1-butene proceed according to the pathway shown in Scheme 1. 1-Butene is protonated by Brønsted acid site to form

Figure 12. Variation in the composition of the products as a function of temperature for the reaction of 1-butene over silicalite-1(NH$_3$). Expressions of compounds and reaction conditions are the same as those in Figure 7.

Scheme 1. Simplified Reaction Pathway of Reaction of 1-Butene over H-ZSM-5 and Silicalite-1

propene reached 39.1 C-wt % at 550 °C, the highest values among those for four silicalite-1 catalysts. The formation of C8+, including alkenes, alkanes, and aromatics was smaller over silicalite-1(NH$_3$) than over silicalite-1.

Over silicalite-1(non-F), the general trend of the changes in composition with temperature was similar to those for the other silicalite-1's. The formation of C8+ was not extended, as compared with that observed for silicalite-1 in the temperature range 350−550 °C, and the formations of aromatics and alkanes were not extended, as compared with those for silicalite-1(HCl) and silicalite-1(NH$_3$) in the temperature range 400−550 °C. The maximum yield of propene over silicalite-1(non-F) reached 31.6 C-wt % at 550 °C, which was a little smaller than those obtained for the other silicalite-1's.

Over H-ZSM-5(80) and H-ZSM-5(280), the changes in the composition with the reaction temperature were between those

2-butyl cation. The 2-butyl cation converts to *trans*- and *cis*-2-butene by deprotonation, octane and dodecene isomers by oligomerization and isobutene by skeletal isomerization. Octene and dodecene isomers undergo cracking to form alkenes. Alkenes undergo hydrogen transfer to form alkanes and aromatics.

Among these reactions, the double-bond isomerization is the easiest reaction. The reaction proceeds at a low temperature. The equilibrium conversions of 1-butene to 2-butenes are 93.1, 87.7, and 83.2% at 100, 200, and 250 °C, respectively.[29] The 1-butene conversions over H-ZSM-5(23) at 100 °C, over silicalite-1(NH$_3$) at 200 °C, and over silicalite-1 at 250 °C were

89, 83, and 83%, respectively. The temperatures at which the conversions closely reached the equilibrium conversions were 100, 200, and 250 °C for H-ZSM-5(23), silicalite-1(NH$_3$), and silicalite-1, respectively.

Because alkanes and aromatics formed to a large extent at a higher temperature over H-ZSM-5(23) possessing strong acid sites, it can be assumed that strong acid sites are required for the hydrogen transfer reaction. The hydrogen transfer reaction forming alkanes and aromatics consists of several steps: a protonation step, an oligomerization step, three hydride transfer steps, three proton transfer steps, one cyclization step, and one ring expansion step in the case of the reaction of 1-butene to butane and xylene (Supporting Information Scheme S1). The proton transfer step may be either to alkenes to form carbocation or to the surface to restore the original Brønsted acid sites. The active sites for the hydrogen transfer have not been studied extensively; however, it is plausible to assume that the existence of strongly acidic sites close to each other promotes the reaction efficiently because the proton transfer steps of the former type and hydride transfer steps involved in the hydrogen transfer are the bimolecular reactions between the molecules formed on acid sites and the carbocations adsorbed on the other acid sites. Accordingly, it is assumed that a high concentration of strong acid sites favors the hydrogen transfer reaction. Although it is not certain which step is the slow step among these steps, the slow step should need strong acid sites.

It is noted for silicalite-1 that the percentage of propene increased with the reaction temperature, even though the percentage of total alkenes did not change much in the temperature range 300–550 °C. A similar tendency was observed for H-ZSM-5(280), silicalite-1(HCl), silicalite-1(NH$_3$), and silicalite-1(non-F). Although the reason for this tendency is not certain, one of the possible reasons is as follows: The alkenes formed by skeletal isomerization, oligomerization, and cracking underwent further skeletal isomerization, oligomerization, and cracking repeatedly. Propene is less reactive than the other alkenes with C4 or higher for cracking because the secondary propyl cation has no β-C–C bond to be cleaved by β-scission. It is plausible that propene tended to remain unreacted and increased its concentration with repeating skeletal isomerization, oligomerization, and cracking of alkenes. The other possibility is a high diffusivity of propene as compared with higher alkenes. Propene formed by cracking in the cavities of silicalite-1 or H-ZSM-5 could be diffused out of the cavities more rapidly as compared with higher alkenes before undergoing further oligomerization and cracking.

2.2.2. Active Sites on H-ZSM-5 and Silicalite-1. It is well established that the Brønsted acid sites of H-ZSM-5 zeolites are the OH groups bridging to Si and Al atoms of the zeolite framework. Ammonia molecules adsorbed on the bridged OH groups are desorbed around 300–500 °C in TPD. These acid sites are strong and catalyze many acid-catalyzed reactions. The active sites of H-ZSM-5(23) for the reaction of 1-butene should be the bridged OH groups. These acid sites catalyzed double-bond isomerization in the temperature range 50–150 °C and above; oligomerization, skeletal isomerization; and cracking at 200 °C and above; and hydrogen transfer reaction at 250 °C and above.

On the surface of silicalite-1, no strongly acidic OH groups were observed. In the TPD of ammonia under the conditions normally employed, no desorption peaks appeared. A trace amount of Al was contained in silicalite-1, which originated

from the raw materials perhaps in fumed silica. The amount of Al in silicalite-1 was 2 orders of magnitude smaller than that in H-ZSM-5(23). The activities of silicalite-1 and H-ZSM-5(23) were also largely different; the conversions of 1-butene at 50 °C were 0% for silicalite-1 and 45% for H-ZSM-5(23). The correlation between the Al content and the activity could not be obtained properly. Although the possibility that the strong acid sites originating from the trace Al act as active sites on silicalite-1 could not be excluded, it is worth considering the other possibility, that weakly acidic OH groups on silicalite-1 act as active sites.

It is known that four types of OH groups exist on the surface of silicalite-1. These are terminal silanol, geminal silanol, vicinal silanol, and nest silanol.[30,31] The strength of these OH groups was reported to be in the order, terminal < germinal < vicinal < nest.[30,31] It was reported that the pK_a of the terminal silanol on silica was 4.9 at room temperature.[32,33] The OH groups on silicalite-1 are assumed to increase their acid strength as the temperature increases and act as Brønsted acid at a high temperature. Actually, the nest silanol groups are recognized to be active sites for an acid-catalyzed reaction of Beckmann rearrangement of cyclohexanone oxime to ε-caprolactam carried out in the temperature range 350–400 °C.[26,29–31]

To examine which is more plausible as active sites for propene formation, strong acid sites originating from a trace amount of Al in silicalite-1 or the surface silanol groups, we treated silicalite-1 with HCl to dealuminate and with NH$_3$ to enrich the surface silanol groups. It is anticipated that if the strong acid sites act as the active sites, the propene yield would be decreased by HCl treatment, and if the surface silanol groups act as active sites, the propene yield would be increased by NH$_3$ treatment.

By HCl treatment, 15% of Al in silicalite-1 was removed. The propene yield at 550 °C over the dealuminated silicalite-1 (silicalite-1(HCl)) was increased to a small extent (34.1 to 35.6 C-wt %). By NH$_3$ treatment, the surface OH groups were enriched, as evidenced by IR. The propene yield at 500 °C over the NH$_3$ treated silicalite-1 (silicalite-1(NH$_3$)) increased to a considerable extent (34.1 to 39.1 C-wt %). These results are in favor of the possibility that silanol groups are relevant to the formation of propene from 1-butene, although it is not certain which types of silanol groups are relevant to the reaction.
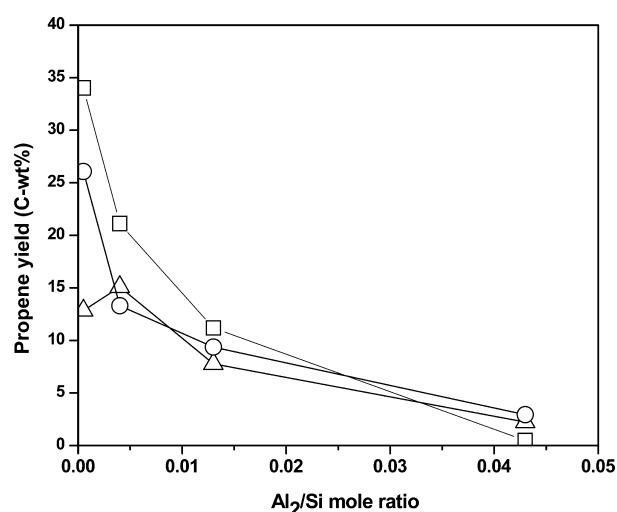
One might argue that because of the presence of fluorine in silicalite-1, acidic properties of silanol groups might be strengthened to show the catalytic activity. The catalytic activity of silicalite-1(non-F) was similar to those of silicalite-1, silicalite-1(HCl), and silicalite-1(NH$_3$) in the sense that the products composed mainly of alkenes and the formations of alkanes and aromatics were small in the temperature range 350–550 °C. The presence of fluorine in silicalite-1 does not much affect the catalytic activity. It is suggested that the silanol groups on silicalite-1 act as an active site without fluorine.

Silicalite-1(non-F) has a morphology different from that of silicalite-1, silicalite-1(HCl), and silicalite-1(NH$_3$), as shown in SEM images (Figure 2). No large crystallites were observed for silicalite-1(non-F). In contrast, large crystallites were observed for silicalite-1, silicalite-1(HCl), and silicalite-1(NH$_3$); however, the crystal size estimated from Scherrer's method was not greatly different for these four silicalite-1's. A large difference between silicalite-1(non-F) and the other silicalite-1's was observed in external surface area. The external surface area was about 20 times larger for silicalite-1(non-F) than for the other silicalite-1's. Regardless of the large differences in morphology,

Table 2. Compositions of the Products in C-wt % for the Reactions of 1-Butene, 1-Pentene, and 1-Hexene over H-ZSM-5(23), H-ZSM-5(80), H-ZSM-5(280), and Silicalite-1 at 550 °C[a]

catalyst	H-ZSM-5(23)			H-ZSM-5(80)			H-ZSM-5(280)			silicalite-1		
	$1\text{-}C_4^=$	$1\text{-}C_5^=$	$1\text{-}C_6^=$	$1\text{-}C_4^=$	$1\text{-}C_5^=$	$1\text{-}C_6^=$	$1\text{-}C_4^=$	$1\text{-}C_5^=$	$1\text{-}C_6^=$	$1\text{-}C_4^=$	$1\text{-}C_5^=$	$1\text{-}C_6^=$
$1\text{-}C_4^=$	0	0	0	0	1.1	1.4	2	2.8	2.4	6.2	3.5	3.3
$2\text{-}C_4^=$	0	0.5	0.4	0.9	2.4	3.0	5.4	6.2	5.4	14.3	7.7	7.2
$i\text{-}C_4^=$	0	0	0.6	1.5	2.3	2.8	2.3	5.9	5.0	13.5	6.9	5.5
$C_2^=$	1.7	3.7	4.9	12.5	8.9	10.1	16.9	12.1	11.0	9.3	7.4	4.9
$C_3^=$	0.5	3.3	4.4	11.2	11.7	14.1	21.1	22.6	20.0	34.1	19.3	39.1
$C_5^=$	0	0	0	0	1.4	1.7	5.1	6.1	5.7	7	48.6	10.6
$C_6^=$	0	0	0	0	0	0	0	0.9	0.8	0.7	1.9	26.6
alkanes	14.8	39.3	45.6	25.4	36.2	33.1	14.7	23.5	17.1	5.1	3.7	1.6
aromatics	50.5	32.7	33.9	40.7	31.5	28.9	22.5	16.6	16.9	5.3	1.0	0.5
C_8+	32.6	20.5	10.4	7.9	4.6	4.9	10.2	3.4	15.9	4.5	0	0.9
$C_2^= + C_3^=$	2.2	7.0	9.3	23.7	20.6	24.2	38.0	34.7	31.0	43.4	26.7	44.0
$C_3^=/C_2^=$ molar ratio	0.2	0.6	0.6	0.6	0.9	0.9	0.8	1.3	1.2	2.4	1.8	6.5

[a]GHSV of 900 h^{-1} for butenes; LHSV of 6 h^{-1} for 1-penetene and 1-hexene; time on-stream, 1 h; total pressure, atmospheric pressure.

Figure 14. Variations in the yield of propene as a function of Al$_2$/Si ratio of catalyst at 550 °C. Propene from reactions of 1-butene (□), 1-pentene (△), and 1-hexene (○) at a GHSV of 900 h^{-1} for 1-butene and LHSV of 6 h^{-1} for 1-pentene and 1-hexene; time on-stream = 1 h; total pressure, atmospheric pressure.
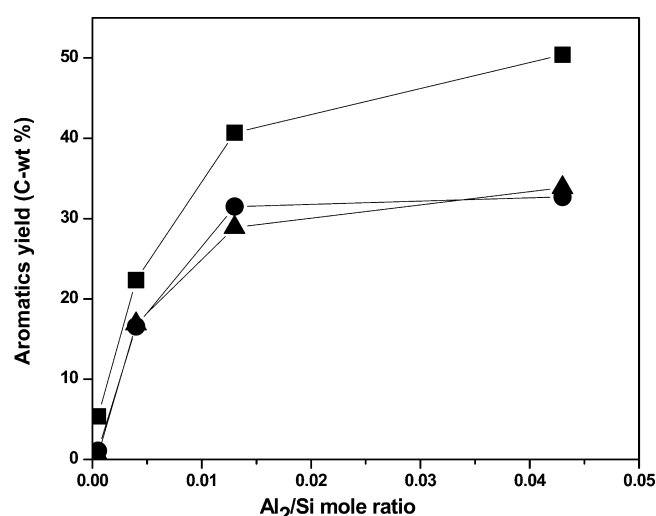
Figure 15. Variations in the yield of aromatics as a function of the Al$_2$/Si ratio of catalyst at 550 °C. Aromatics from reactions of 1-butene (■), 1-pentene (▲), and 1-hexene (●). The reaction conditions are the same as those for Figure 14.

crystal size, and external surface area among silicalite-1(non-F) and other silicalite-1's, the activity and selectivity in the reaction of 1-butene were similar for all silicalite-1 catalysts. The activity and selectivity are governed neither by morphology, diffusion in the cavities, or F-content, nor by concentration of the terminal silanol groups, which are estimated to be high for silicalite-1(non-F) having a large external surface area. It is suggested that the silanol groups other than the terminal silanol groups act as catalytically active sites.

A hydrogen transfer reaction occurred above 250 °C for H-ZSM-5(23), but a hydrogen transfer reaction scarcely occurred, even at 550 °C, for silicalite-1. The high yield of propene over silicalite-1 results from the fact that silicalite-1 possesses only weak acid sites that can promote isomerization, oligomerization, and cracking, but cannot promote a hydrogen transfer reaction. The acid sites of H-ZSM-5 zeolites are strong enough to promote a hydrogen transfer reaction in the temperature range 300−550 °C, by which the formed alkenes are consumed to form alkanes and aromatics.

2.2.3. Reactions of 1- Pentene and 1-Hexene. The catalytic performances of H-ZSM-5(23), H-ZSM-5(80), H-ZSM-5(280),

and silicalite-1 were examined for the reactions of 1-pentene and 1-hexene to see whether the catalytic performances observed for 1-butene were also observed for other alkenes. The reactions were carried out at 550 °C, and the results are summarized in Table 2, in which the results of 1-butene reaction are included for comparison.

The product distributions for the reactions of 1-pentene and 1-hexene were essentially the same as those observed for the reaction of 1-butene. Over silicalite-1, the yield of propene was the highest for the reactions of both 1-pentene and 1-hexene except for the reaction of 1-pentene, in which H-ZSM-5(280) showed a slightly higher yield (22.6 C-wt %) than silicalite-1 (19.3 C-wt %). In particular, 39.1 C-wt % of propene yield was obtained for the 1-hexene reaction. The formations of alkanes and aromatics were very small: <6 wt %. Over H-ZSM-5(23), on the other hand, the yields of propene were less than 5 wt % from both 1-pentene and 1-hexene. Large amounts of alkanes and aromatics were formed from these reactants; the yields of them exceeded 30 C-wt %.

On the last line in Table 2, the propene/ethylene molar ratios are included. It is noted that the ratio increased with an

increase in the Si/Al_2 molar ratio of the catalyst. Silicalite-1 gave the highest ratio of propene/ethylene. In particular, a high ratio of 6.5 was observed for the 1-hexene reaction over silicalite-1. The formation of ethylene involves primary carbocation as an intermediate, which needs strong acid sites. The formation of ethylene is assumed to be suppressed over silicalite-1 because of the absence of strong acid sites.

The features of the catalysts became clearly seen when we plotted the yields of propene and aromatics in the reactions of 1-butene, 1-pentene, and 1-hexene against a reciprocal of Si/Al_2 ratio (Al_2/S) as shown in Figures 14 and 15. The propene yields increased with a decrease in the Al_2/Si ratio, except for the reaction of 1-pentene over H-ZSM-5(280) and silicalite-1 (Figure 14). In contrast to the yields of propene, the yields of aromatics increased with an increase in the Al_2/Si ratio for the reactions of all alkenes (Figure 15). As the number of strong acid sites increased, the aromatic formation increased, and the propene formation decreased. The absence of strong acid sites maximized the propene formation.

CONCLUSIONS

Silicalite-1 acts as an efficient catalyst for the formation of propene by the reaction of light alkenes because of the presence of weak acid sites and the absence of strong acid sites. It was proposed that the weakly acidic silanol groups on silicalite-1 act as active sites for the production of propene, starting with protonation of alkenes to form carbenium ions, followed by oligomerization and cracking. Strongly acidic bridged OH groups on H-ZSM-5 catalysts promote hydrogen transfer of alkenes to form aromatics and alkanes, which lowers the yield of propene. The absence of strongly acidic sites on silicalite-1 prevents the alkenes from further converting to alkanes and aromatics by hydrogen transfer. The silicalite-1 treated with ammonia to enrich the surface silanol groups exhibited the maximum propene yield of 39.1 C-wt % from 1-butene at 550 °C.

ASSOCIATED CONTENT

Ⓢ Supporting Information

Blank test, numerical data for Figures 7−13, and Scheme for hydrogen transfer. This material is available free of charge via the Internet at http://pubs.acs.org.

AUTHOR INFORMATION

Corresponding Author
*Phone: +966 13 8602029. E-mail: skhattaf@kfupm.edu.sa.

Notes
The authors declare no competing financial interest.

ACKNOWLEDGMENTS

REFERENCES

(1) Liu, H. J.; Zhang, L.; Li, X. J.; Huang, S. J.; Liu, S. L.; Xin, W. J.; Xie, S. J.; Xu, L. Y. *J. Nat. Gas Chem.* **2009**, *18*, 331−336.
(2) Zhao, Q. F.; Chen, S. L.; Gao, J. S.; Xu, C. M. *Transition Met. Chem. (N.Y.)* **2009**, *34*, 621−627.
(3) Zhu, X.; Li, X.; Xie, S.; Liu, S.; Xu, G.; Xin, W.; Huang, S.; Xu, L. *Catal. Surv. Asia* **2009**, *13*, 1−8.
(4) Plotkin, J. S. *Catal. Today* **2005**, *106*, 10−14.
(5) Lu, J.; Zhao, Z.; Xu, C.; Duan, A.; Zhang, P. *Catal. Lett.* **2006**, *109*, 65−70.
(6) Zhu, X.; Liu, S.; Song, Y.; Xu, L. *Catal. Lett.* **2005**, *103*, 201−210.
(7) Zhu, X.; Liu, S.; Song, Y.; Xie, S.; Xu, L. *Appl. Catal., A* **2005**, *290*, 191−199.
(8) Xue, N.; Nie, L.; Fang, D.; Guo, X.; Shen, J.; Ding, W.; Chen, Y. *Appl. Catal., A* **2009**, *352*, 87−94.
(9) Zhao, G.; Teng, J.; Zhang, Y.; Yue, Y.; Chen, Q.; Tang, Y. *Appl. Catal., A* **2006**, *299*, 167−174.
(10) Sazama, P.; Dedecek, J.; Gabova, V.; Wichterlova, B.; Spoto, G.; Bordiga, S. *J. Catal.* **2008**, *254*, 180−189.
(11) Zhu, X.; Liu, S.; Song, Y.; Xu, L. *Appl. Catal., A* **2005**, *288*, 134−142.
(12) Vora, B.; Marker, T. L.; Barger Enhanced Light Olefin Production, U.S. Patent 6,049,017, April 11, 2000.
(13) Tang, X.; Zhou; Qian, W.; Wang, D.; Jin, Y.; Wei, F. *Catal. Lett.* **2008**, *125*, 380−385.
(14) Lin, L.; Qiu, C.; Zhuo, Z.; Zhang, D.; Zhao, S.; Wu, H.; Liu, Y.; He, M. *J. Catal.* **2014**, *309*, 136−145.
(15) Zeng, P.; Liang, Y.; Ji, S.; Shen, B.; Liu, H.; Wang, B.; Zhao, H.; Li, M. *J. Energy Chem.* **2014**, *23*, 193−200.
(16) Epelde, E.; Gayubo, A. G.; Olazar, M.; Bilbao, J.; Agyayo, A. T. *Ind. Eng. Chem. Res.* **2014**, *53*, 4614−4622.
(17) Colombo, F., Alberti, G., Padovan, M., Paparatto, G., Contessa, S. Process for the Conversion of Linear Butenes to Propylene. Eur. Pat. EP 0109060, March 11, 1987.
(18) Aubert, E.; Porcher, F.; Souhassou, M.; Petricek, V.; Lecomte, C. *J. Phys. Chem. B* **2002**, *106*, 1110−1117.
(19) Fyfe, C. A.; Darton, R. J.; Mowatt, H.; Lin, Z. S. *Microporous Mesoporous Mater.* **2011**, *144*, 57−66.
(20) Katada, N.; Igi, H.; Kim, J.-H.; Niwa, M. *J. Phys. Chem. B* **1997**, *101*, 5969−5977.
(21) Treacy, M. M. J.; Higgins, J. B.; von Ballmoos, R. *Collection of Simulated XRD Powder Diffraction Patterns for Zeolites*, 4th revised ed.; Elsevier: London, 2001; p 237.
(22) Baerlocher, C. H.; Meier, W. M.; Olson, D. H. *Atlas of Zeolite Framework*, 6th ed.; Elsevier Science: Amsterdam, 2007; p 212.
(23) Hardenberg, T. A. J.; Mertens, L.; Mesman, P.; Muller, H. C.; Nicolaides, C. P. *Zeolite* **1992**, *12*, 685−689.
(24) Feng, F.; Balkus, K. J., Jr. *Microporous Mesoporous Mater.* **2004**, *69*, 85−96.
(25) Parry, E. P. *J. Catal.* **1963**, *2*, 371−379.
(26) Emeis, C. A. *J. Catal.* **1993**, *141*, 347−354.
(27) Hoelderich, W. F.; Roeseler, J.; Heitmann, G.; Liebens, A. T. *Catal. Today* **1997**, *37*, 353−366.
(28) Kadata, N.; Niwa, M. *Catal. Surv. Asia* **2004**, *8*, 161−170.
(29) Ono, Y.; Hattori, H. *Solid Base Catalysis*; Springer Series in Chemical Physics 101; Springer: Heidelberg, 2011; pp 42−47.
(30) Heitmann, G. P.; Dahlhoff, G.; Hoelderich, W. F. *J. Catal.* **1999**, *186*, 12−19.
(31) Ichihashi, H.; Ishida, M.; Shiga, A.; Kitamura, M.; Suzuki, T.; Suenobu, K.; Sugita, K. *Catal. Surv. Asia* **2003**, *7*, 261−270.
(32) Ishida, M.; Suzuki, T.; Ichihashi, H.; Shiga, A. *Catal. Today* **2003**, *87*, 187−194.
(33) Ong, S. W.; Zhao, X. L.; Eisenthal, K. B. *Chem. Phys. Lett.* **1992**, *192*, 327−335.